NANOSYSTEMS: PHYSICS, CHEMISTRY, MATHEMATICS, 2021, 12 (3), P. 336–345

Synthesis of core-shell titanium dioxide nanoparticles with water-soluble shell of poly(methacrylic acid)

E. L. Krasnopeeva[1,2], E. Yu. Melenevskaya[1], O. A. Shilova[2], A. M. Nikolaev[2], A. V. Yakimansky[1]

[1]Institute of Macromolecular Compounds, Russian Academy of Sciences, St. Petersburg, Russia
[2]Grebenshchikov Institute of Silicate Chemistry, Russian Academy of Sciences, St. Petersburg, Russia

opeeva@gmail.com

PACS 61.46.+w, 68.47.Pe **DOI 10.17586/2220-8054-2021-12-3-336-345**

The article is devoted to the covalent modification of the surface of titanium dioxide nanoparticles with polymethacrylic acid using the method of controlled atom transfer radical polymerization. For the first time, core-shell titanium dioxide nanoparticles with water-soluble shell of poly(methacrylic acid) were obtained.

Keywords: modification of nanoparticles, titanium dioxide, controlled radical polymerization, polymethacrylic acid, core-shell nanoparticles.

Received: 2 December 2020

Revised: 9 April 2021

1. Introduction

In the recent years, nanosized titania and titania-based nanocomposites have become increasingly popular materials in the industrial-scale manufacturing of many products, agriculture, environmental science, and power engineering due to their photocatalytic [1–6], photoluminescent [7,8], semiconductor [9–11], pigment [12], and biological [13–15] properties. In particular, titanium dioxide nanoparticles are widely used in agriculture for the photocatalytic decomposition of pesticides [16–31], solar energy-assisted photocatalytic water purification (review [16] and references therein), plant disease control [32–34]. One of the most important application areas of TiO_2 nanoparticles in agriculture is treatment of crop seeds aimed at accelerating seed germination and crop vegetation [35–40]. The possibility of this practical application of titanium dioxide is related to its capability for photocatalytic activation of oxygen, which yields reactive oxygen species such as peroxide and hydroxide radicals and ions. As a result, stress tolerance of seeds is enhanced, their ability to absorb water and oxygen increase [36]. Besides, treatment of seeds with titanium dioxide nanoparticles leads to enhanced nitrogen binding by plants, increase in chlorophyll and protein contents in plants [38].

In order to increase efficiency of TiO_2-based photocatalytic systems, it is necessary to use this substance in the form of stabilized aqueous dispersions (which are generated, for instance, upon interaction with triethanolamine [41]), or in the form of core-shell nanoparticles with TiO_2 core and a water-soluble shell. The most promising synthetic method for these core-shell structures consists in modifying titanium dioxide nanoparticle surfaceswith covalently grafted chains of water-soluble hydrophilic polymers. To date, a relatively large number of works devoted to modification of TiO_2 nanoparticles with various polymers have been published. The most common method is controlled atom transfer radical polymerization (ATRP) of vinyl monomers involving α-Br-ester groups immobilized on nanoparticle surface [42–54]. In most cases, this immobilization is preceded by modification of TiO_2 surface with amino groups in the process of treatment of nanoparticles with 3-aminopropyltriethoxysilane [42, 48–51, 53] or dopamine [43]. Then, the obtained nanoparticles are treated with bromoanhydrides of 2-bromopropionic or 2-bromo-isobutyric acids [42, 43, 48–51, 53], which results in immobilization of ATRP-initiating α-Br-ester groups on nanoparticle surface. In some cases, TiO_2 nanoparticles are immediately treated with 2-Br-isobutyroyl bromide [44].

It should be noted that there are virtually no literature data on modification of TiO_2 nanoparticle surfaces with water-soluble polymers. A small number of published papers report the synthesis of titanium dioxide and zinc oxide nanoparticles modified with poly(N,N-diethylaminoethyl methacrylate), which were used as nanocontainers for anticancer preparations [44]. Titanium dioxide nanoparticles modified with ionized poly(styrene sulfonic acid) were used as ion exchangers for Ag^+; the products were intended for applications as TiO_2/Ag binary nanocomposite photocatalysts [45] and one of components of proton-conducting membranes [54]. There are also papers reporting the synthesis of TiO_2 nanoparticles modified with poly(oligoethylene glycol) methacrylate [47] and poly(N-isopropyl acrylamide); the latter demonstrate self-flocculation in aqueous medium at temperatures above low critical solution temperature of poly(N-isopropyl acrylamide) [51,52]. In addition, block copolymers of styrene and acrylic acid were used as micellar nanoreactors for the synthesis of TiO_2 nanoparticles and stabilization of TiO_2 aqueous dispersions [55].

In the present work, we synthesized core-shell TiO_2 nanoparticles modified with water-soluble poly(methacrylic acid) for the first time. The two-stage grafting method described above was used for immobilization of 2-Br-isobutyrate groups on the surface of titanium dioxide; the method involved successive treatment of nanoparticles with 3-aminopropyltriethoxysilane and 2-Br-isobutyroyl bromide. Then, the obtained TiO_2-based macroinitiators were used for polymerization of *tert*-butyl methacrylate (TBMA) by ATRP. The prepared core-shell TiO_2@PTBMA nanoparticles with grafted PTBMA chains were subjected to acidic hydrolysis; ester groups of the grafted chains were converted to carboxylategroups, and TiO_2@PMAA core-shell nanoparticles with poly(methacrylic acid) shells were obtained. In order to determine lengths of the grafted chains, they were isolated by selective alkaline hydrolysis of ester bonds that connect polymer chains to TiO_2 surface; molecular masses and molecular mass distributions were estimated by size exclusion liquid chromatography (SEC).

The structure of nanoparticles at all stages of synthesis was confirmed by IR spectroscopy and solid state ^{13}C NMR spectroscopy.

2. Experimental: materials

3-Aminopropyltriethoxysilane (99 %, Acros Organics), N,N-dimethylformamide (DMF) (reagent grade, Vekton, Russia), and *N*, *N*, *N*', *N*", *N*"-pentamethyldiethylenetriamine (PMDETA) (99 %, Aldrich) were used without additional purification. Methylene chloride (reagent grade, Vekton, Russia) and toluene (analytical grade, Vekton, Russia) were dried by heating over anhydrous calcium hydride (99.9 %, Aldrich), then distilled under vacuum. The ionic liquid (1-butyl-3-methylimidazolium chloride (BMIMCl) ($\geq$98.0 % (Aldrich)), glacial acetic acid (reagent grade, Vekton, Russia), trifluoroacetic acid (99 %, Aldrich), copper (I) bromide (99.999 %, Aldrich), 2-bromo-isobutyroyl bromide (98 %, Aldrich) were used without additional purification. *Tert*-butyl methacrylate (TBMA) (98 %, Aldrich) was twice distilled under vacuum before use, commercial TiO_2 rutile nanopowder (Plasmotherm) was used for the modification.

3. Experimental: methods

3.1. TiO_2 nanoparticles

SEM image of particles is presented in Fig. 1. According to these data, the particles have the size of 100 – 300 nm, being characterized by the specific surface area (SSA) of $\sim$ 13 m^2/g and specific pore volume of 0.044 cm^3/g [56].

X-Ray diffraction of particles is presented in Fig. 2.

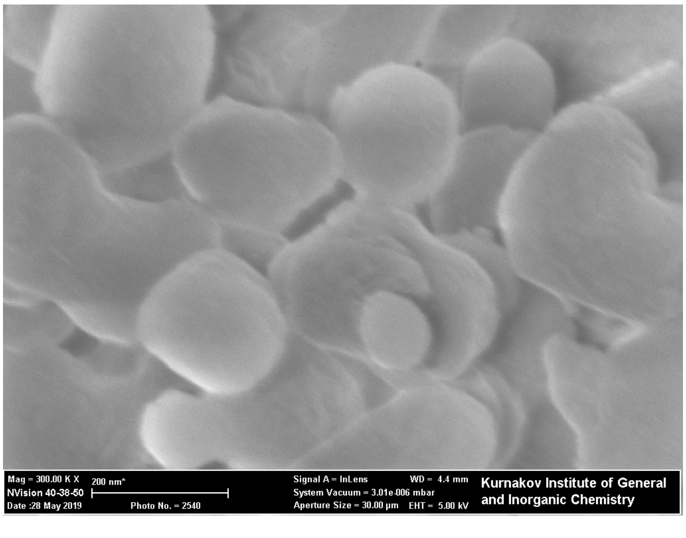

FIG. 1. SEM image of TiO_2 nanoparticles

3.2. Synthesis of TiO_2 nanoparticles modified with 3-aminopropyltriethoxysilane (APTES)

Titanium dioxide particles (0.73 g) were annealed under vacuum at 120 °C for 4 h in order to remove physically adsorbed water [57]. Then the product was cooled down to room temperature, and DMF (10 mL) was recondensed into the reaction vessel, and the mixture was subjected to ultrasound treatment for 30 min. Then the mixture was degassed thrice, and argon was passed through the system; APTES (0.5 mL) was added at cooling in an ice bath and at constant stirring. The mixture was left to stand for 24 h at constant agitation under anargon atmosphere at room temperature.

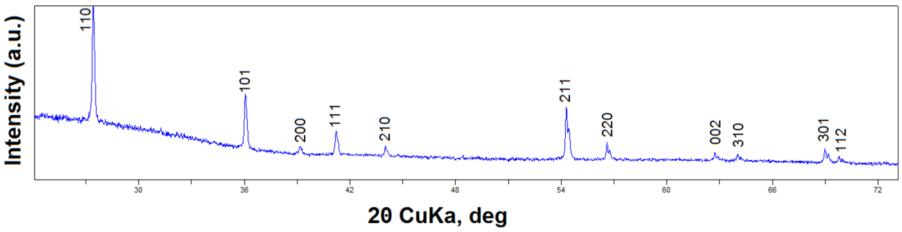

FIG. 2. X-Ray diffractogram of the TiO_2

The particles were isolated by centrifugation, washed thrice with DMF and thrice with methylene chloride. Yield: 0.74 g.

3.3. Synthesis of TiO_2-APTES-BiB macroinitiators based on TiO_2-APTES

Titanium dioxide nanoparticles modified with APTES (TiO_2-APTES, 0.5 g) were heated at 110 °C under vacuum for 2 h. Dry toluene (25 mL) was recondensed into the reaction flask; the mixture was degassed thrice, andargon was passed through the system; then 2-bromo-isobutyroyl bromide (BiB, 2 mL) was added. The reaction mixture was exposed at room temperature and constant stirring for 24 h. The product was precipitated into deionized water and washed thrice with subsequent centrifugation. The final product was obtained in the form of white powder. Yield: 0.83 g.

3.4. Synthesis of TiO_2-APTES-BiB-PTBMA core-shell nanoparticles with poly(*tert*-butylmethacrylate) (PTBMA) shells

The initiator (0.2 g) was put into the reaction flask together with 10 g of the ionic liquid (butyl-methyl imidazolium chloride), heated to 80 °C at constant stirring, degassed and subjected to ultrasound treatment for 30 min. Then, argon was passed through the flask; CuBr (0.063 g) and PMDETA (0.7 mL) were added. Then preliminarily distilled TBMA was added in the amounts indicated below. The mixture was exposed at 80 °C with constant agitation for 24 h. The synthesized particles were precipitated into excess distilled water and dried in air. The final product was obtained in the form of white powder.

The following samples containing various amounts of PTBMA were synthesized by addition of 7.5, 2.5, and 1 mL of TBMA: TiO_2-APTES-BiB-PTBMA-1, TiO_2-APTES-BiB-PTBMA-2, and TiO_2-APTES-BiB-PTBMA-3, respectively.

3.5. Elimination of grafted PTBMA chains by alkaline hydrolysis of TiO_2-APTES-BiB-PTBMA core-shell nanoparticles

The particles were put into 2 wt. % solution of KOH in methanol at 65 °C and exposed for 16 h. Linear PTBMA was precipitated into the methanol:water mixture and dried until constant weight was achieved.

3.6. Synthesis of TiO_2-APTES-BiB-PMAA core-shell nanoparticles with poly(methacrylic acid) (PMAA) shells

The synthesized TiO_2-APTES-BiB-PTBMA-1, TiO_2-APTES-BiB-PTBMA-2, and TiO_2-APTES-BiB-PTBMA-3 samples were dissolved in minimal amount of methylene chloride; trifluoroacetic acid (small excess) was added, then the mixture was exposed for 24 h at room temperature and constant stirring. The formed precipitate was washed with dichloromethane until neutral pH was reached, and then dried in air. Titanium dioxide particles modified with water-soluble poly(methacrylic acid) chains of various lengths (TiO_2-APTES-BiB-PMAA-1, TiO_2-APTES-BiB-PMAA-2, and TiO_2-APTES-BiB-PMAA-3) were obtained.

3.7. X-Ray diffraction

X-Ray diffraction was carried out using Rigaku MiniFlexII diffractometer with CuKα radiation in the 2θ range 5 – 75 °, with step 0.02° at 5 °/min speed. Crystal scattering domain (CSD) length was calculated with Debye–Scherrer formula using 110 reflections.

3.8. IR spectroscopy

IR Fourier transform spectra were obtained with the aid of an IRAffinity-1S spectrometer (Shimadzu) equipped with a Quest attenuated total reflectance attachment (Specac) (diamond prism, spectral range 7800 – 400 cm^{-1}).

3.9. NMR spectroscopy

Solid state ^{13}C NMR spectra were recorded using a Bruker Avance 400 SB instrument (1H: 400 MHz).

3.10. Size exclusion chromatography

The samples were analysed with the aid of an Agilent-1260 Infinity chromatography setup equipped with two columns packed with PLgel MIXED-C sorbent (column dimensions: 7.5×300 mm; sorbent particle size: 5 μm). Elution proceeded in isocratic regime; dimethylformamide was used as an eluent. Molecular masses and polydispersity parameters were measured by multidetector gel permeating chromatography. Characteristics of polymers were determined from the data of refractometric and viscosimetric detectors used in combination with a light scattering detector, which makes it possible to manage without calibration standards.

3.11. Scanning electron microscopy

The SEM studies were performed with the aid of a Carl Zeiss N Vision 40 instrument at an accelerating voltage of 1 kV and magnification of up to ×300000.

3.12. Thermogravimetry

A DTG-60 setup (Shimadzu, Kyoto, Japan) was used for thermogravimetric (TGA) analysis to determine the amount of OH-groups chemically bound to the surface of TiO_2 nanoparticles, the samples being heated to 600 °C at a rate of 5 °C/min in air flow (80 mL/min).

4. Results and discussion

TiO_2 nanoparticles were studied by the TGA method in order to determine the amount of surface OH-groups bound covalently to Ti atoms. According to the procedure described in [57], the following equation was used to this aim:

$$\#\mathrm{OH}/\mathrm{nm}^2 = 0.625 \times \frac{2\,(\Delta W_{T_1\to T_2})\,N_A}{SSA \times MW_{\mathrm{H_2O}}}, \tag{1}$$

where $\Delta W_{T_1\to T_2}$ is the weight loss fraction upon heating the sample from $T_1 = 120$ °C (the annealing temperature at which physically adsorbed water is removed) to $T_2 = 600$ °C (the temperature at which no chemically bound OH-groups remain on the surface of titania nanoparticles [57]), N_A is Avogadro number, $MW_{\mathrm{H_2O}}$ is the molecular weight of water. As may be found from the TGA curve presented in Fig. 3, $\Delta W_{T_1\to T_2} \approx 0.0092$. Then, according to formula (1) with $SSA = 13$ m^2/g, the surface density of chemically bound OH-groups, $\#\mathrm{OH}/\mathrm{nm}^2 = 29.4$ nm^{-2}. This value corresponds to $\sim 3.822 \cdot 10^{20}$ chemically bound surface OH-groups per 1 g of TiO_2 nanoparticles.

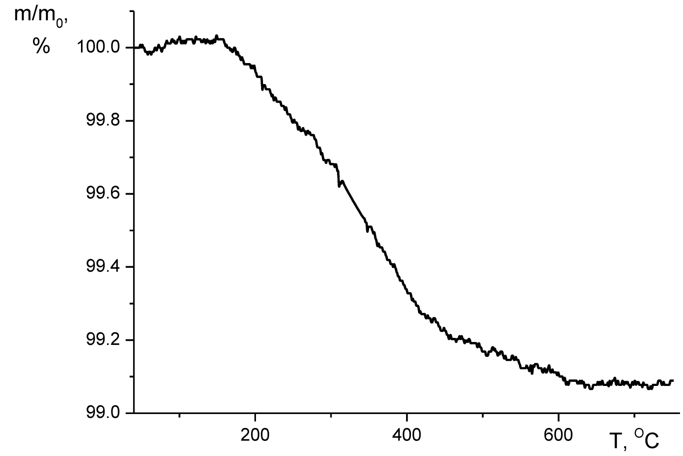

FIG. 3. TGA curve of the powder of TiO_2 nanoparticles

The scheme of the synthesis of TiO_2-APTES-BiB-PMAA core-shell particles with titanium dioxide cores and poly(methacrylic acid) shells included several stages; the synthesis scheme is presented in Fig. 4.

At the first stage, titanium dioxide nanoparticles were treated with APTES in order to graft primary amino groups onto nanoparticles' surface. The taken amount of APTES (0.5 g) corresponds to an approximately 5-fold molar excess

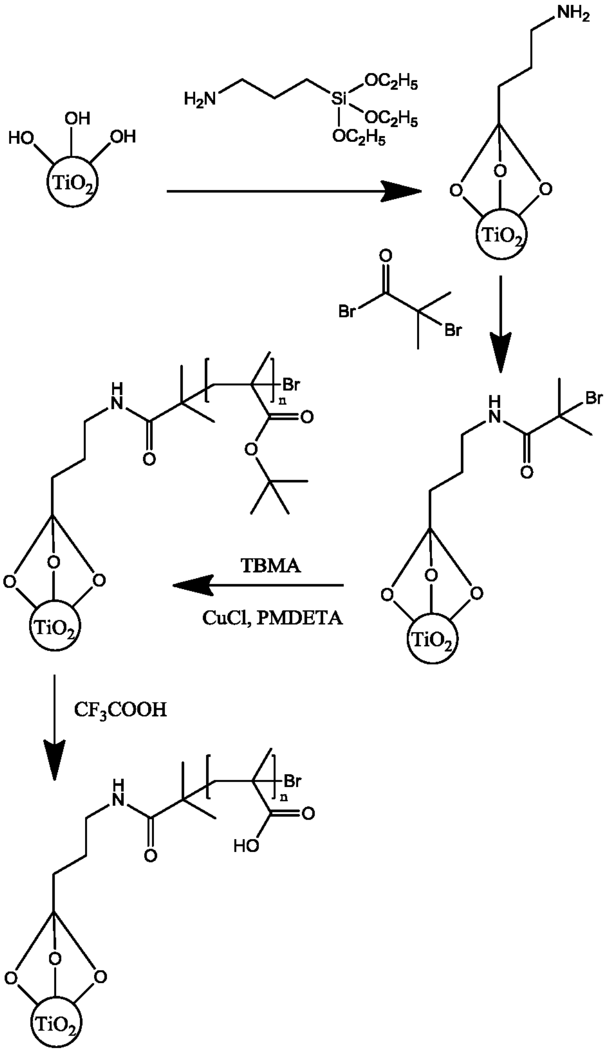

FIG. 4. Scheme of the synthesis of TiO_2-APTES-BiB-PMAA core-shell particles with titanium dioxide cores and poly(methacrylic acid) shells

of APTES with respect to chemically bound surface OH-groups in the taken amount of annealed TiO_2 nanoparticles (0.73 g). The presence of amino groups on the surface of the synthesized particles is confirmed by comparison of ^{13}C NMR spectra of the initial titanium dioxide nanoparticles (Fig. 5a) and the nanoparticles treated with APTES (Fig. 5b). The spectrum of the initial nanoparticles presented in Fig. 5a indicates that they have pure surface, i.e. there are no carbon-containing groups or compounds on TiO_2.

Meanwhile, the spectrum of TiO_2-APTES nanoparticles contains the signals attributed to carbon atoms of aminopropyl groups near 10, 25 and 45 ppm. In addition, the presence of surface amino groups is confirmed by comparison of IR spectra of the initial TiO_2 nanoparticles before and after treatment with APTES (Fig. 6). The following bands appear in the spectra of APTES derivatives: (i) wide bands in the region 1560 – 1570 cm^{-1} attributed to deformation vibrations of primary amino groups [58]; (ii) C–N stretching vibration band of APTES at 1323 cm^{-1} [58]; (iii) the bands near 1140 cm^{-1} assigned to valence vibrations of C–N bond in primary amines [59].

At the second stage, surface amino groups of TiO_2-APTES nanoparticles were acylated with 2-bromo-isobutyroyl bromide to graft 2-bromo-isobutyrate groups onto nanoparticles' surface; these fragments are able to initiate controlled atom transfer radical polymerization. ^{13}C NMR spectrum of the resulting TiO_2-APTES-BiB nanoparticles is presented in Fig. 5c. Comparison of this spectrum with NMR spectrum of TiO_2-APTES (Fig. 5b) demonstrates that the former-contains new signals attributed to methyl carbon atoms (32 ppm), quaternary carbon atoms (52 ppm), and carbonyl atoms in 2-bromo-isobutyrate fragments (170 – 180 ppm). Thus, the ^{13}C NMR spectroscopy data confirm successful preparation of TiO_2-APTES-BiB nanoparticles with surface 2-bromo-isobutyrate groups.

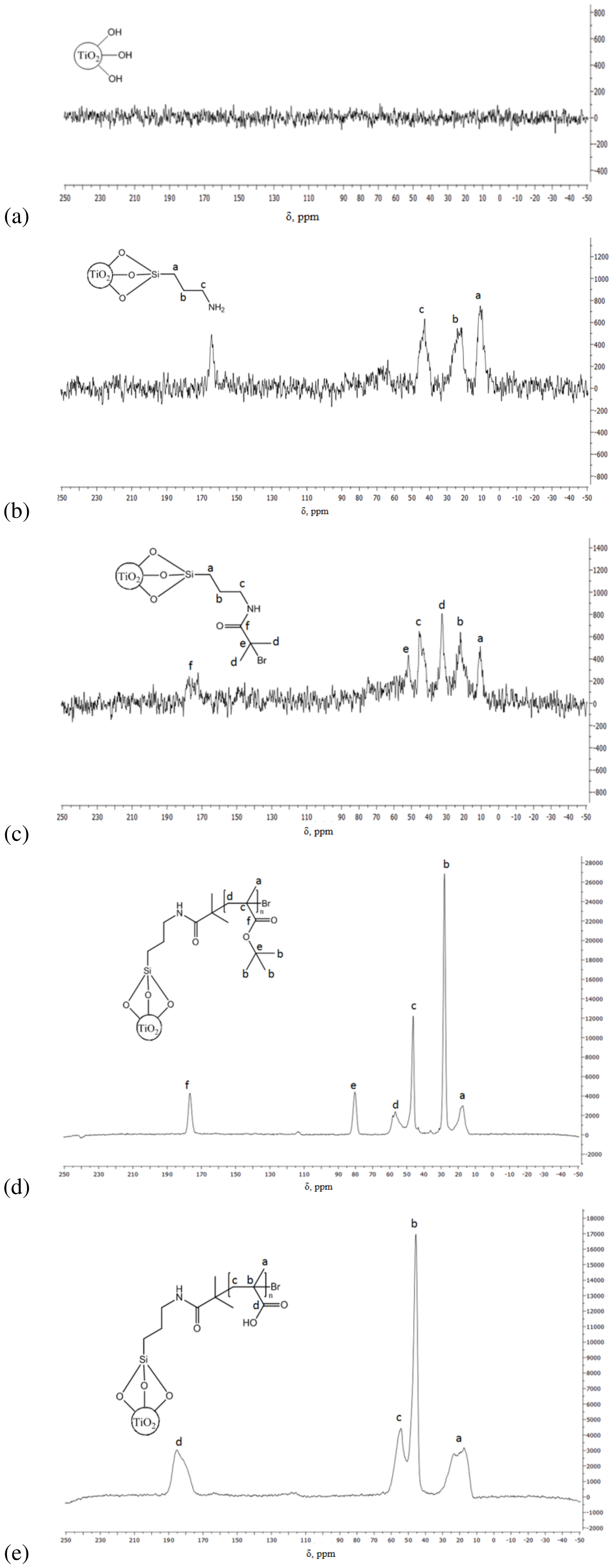

FIG. 5. Solid state ^{13}C NMR spectra of the initial titanium dioxide (a), TiO_2-APTES (b), TiO_2-APTES-BiB (c), TiO_2-APTES-BiB-PTBMA (d) and TiO_2-APTES-BiB-PMAA particle (e)

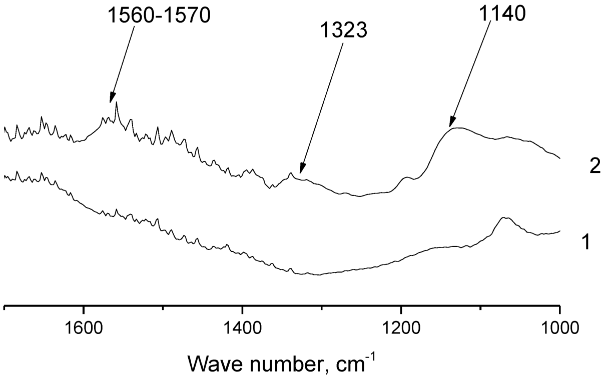

FIG. 6. IR spectra of the initial titanium oxide (1) and TiO_2-APTES nanoparticles (2)

The synthesized TiO_2-APTES-BiB nanoparticles were used in polymerization of *tert*-butyl methacrylate according to ATRP mechanism. The TiO_2-APTES-BiB-PTBMA nanoparticles were synthesized; their ^{13}C NMR spectrum (Fig. 5d) virtually coincides with that of poly(*tert*-butyl methacrylate). It includes signals related to all PTBMA carbon atoms: methylene group ($\sim$ 55 ppm) and α-carbon atom ($\sim$ 45 ppm) of PTBMA backbone, methyl group at α-carbon ($\sim$ 18 ppm), signals of carbonyl atoms ($\sim$ 180 ppm), quaternary carbon atoms ($\sim$ 80 ppm) and methyl carbon atoms ($\sim$ 28 ppm) of side ester groups. It should be noted that signals of TiO_2-APTES-BiB macroinitiator cannot be registered due to its extremely low amount in TiO_2-APTES-BiB-PTBMA samples.

The grafted PTBMA chains were eliminated from TiO_2-APTES-BiB-PTBMA nanoparticles in the process of alkaline hydrolysis, which destructs the ester bonds connecting polymer chains to macroinitiator fragments. Conditions of alkaline hydrolysis were selected so as to prevent transformation of side ester fragments of PTBMA [60]. The isolated linear PTBMA was analyzed by multidetector size exclusion liquid chromatography with the so-called triple detection (a combined analysis of the data provided by refractometric, viscosimetric and light scattering detectors [61]). It was found that the isolated PTBMA chains have the following characteristics: $M_n = 70000$, $M_w = 120000$, $M_w/M_n = 1.7$. Thus, the PTBMA chains grafted onto the surface of titanium dioxide nanoparticles are long (polymerization degree about 500) and have relatively narrow molecular mass distributions.

At the last synthesis stage, TiO_2-APTES-BiB-PTBMA nanoparticles were subjected to "dry" acidic hydrolysis that affected side ester groups of PTBMA chains. Hydrolysis proceeded under the action of anhydrous trifluoroacetic acid and was accompanied by release of gaseous isobutylene and transformation of ester groups into carboxylic fragments. As a result, we obtained TiO_2-APTES-BiB-PMAA nanoparticles with water-soluble poly(methacrylic acid) shells, their polymerization degree being the same as that of the initial PTBMA chains. ^{13}C NMR spectrum of these nanoparticles given in Fig. 5e confirms the presence of poly(methacrylic acid) in the shell. Thus, the spectrum contains the signals attributed to methylene group atoms ($\sim$ 55 ppm) and α-carbon atoms($\sim$ 45 ppm) of PMAA backbone, the signals of methyl group at α-carbon atom ($\sim$ 20 ppm) and carboxylic carbon atom ($\sim$ 185 ppm). At the same time, there are no peaks related to quaternary carbon atoms and methyl carbon atoms of side ester groups, which indicates complete transformation of TiO_2-APTES-BiB-PTBMA into TiO_2-APTES-BiB-PMAA.

According to the polymerization degree of $\sim$ 500 of PMAA chains in the shell of TiO_2-APTES-BiB-PMAA particles, the shell is $\sim$ 125 nm thick, taking into account that the monomer unit length of PMAA side chains is $\sim$ 0.25 nm. The UV spectrum of the synthesized TiO_2-APTES-BiB-PMAA nanoparticles in water solution is presented in Fig. 7.

As seen from Fig. 7, the spectrum shows a typical absorption of TiO_2 cores below 400 nm [62].

5. Conclusions

Modification of nanoparticles surface with polymers is of great interest for various practical applications. The obtained TiO_2-APTES-BiB-PMAA core-shell nanoparticles with a water-soluble shell can be used, in particular, for treatment of agricultural crop seeds with the purposes of enhancing their germination and increasing growth rate. Each nanoparticle contains photocatalytically active core of titanium dioxide that increases photosynthesis efficiency and poly(methacrylic acid) shell providing solubility of the product in water. It should be noted that the synthesis of titanium dioxide nanoparticles with grafted poly(methyl methacrylate) chains has been described in the literature [63]. However, water-soluble shells of poly(methacrylic acid) were grafted onto the surface of TiO_2 nanoparticles for the first time.

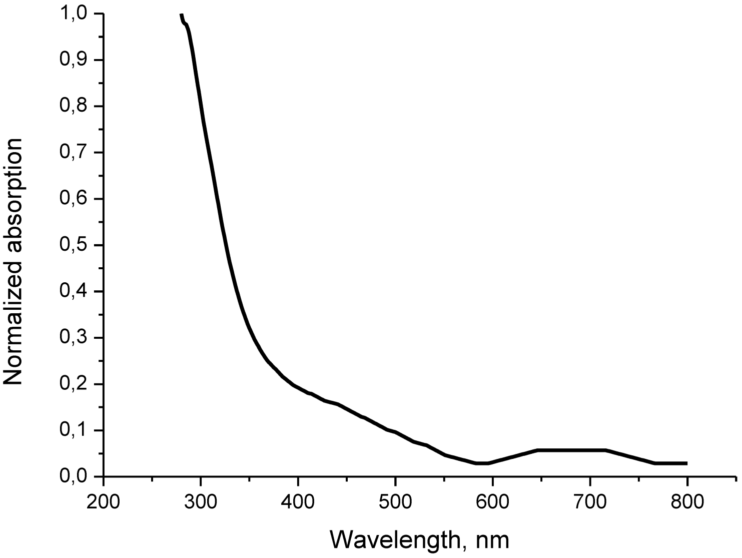

FIG. 7. UV spectrum of TiO_2-APTES-BiB-PMAA nanoparticles in water

Acknowledgements

The work is supported by the Russian Science Foundation (Project No. 19-13-00442).

References

[1] Byrne C., Subramanian G., Pillai S.C. Recent advances in photocatalysis for environmental applications. *Journal of Environmental Chemical Engineering*, 2018, **6**, P. 3531–3555.

[2] Colmenares J.C., Varma R.S., Lisowski P. Sustainable hybrid photocatalysts: titania immobilized on carbon materials derived from renewable and biodegradable resources. *Green Chemistry*, 2016, **18**, P. 5736–5750.

[3] Krasilin A.A., Bodalyov I.S., et al. On an adsorption/photocatalytic performance of nanotubular $Mg_3Si_2O_5(OH)_4$/TiO_2 composite. *Nanosystems: Physics, Chemistry, Mathematics*, 2018, **9**, P. 410–416.

[4] Kolesnik I.V., Lebedev V.A., Garshev A.V. Optical properties and photocatalytic activity of nanocrystalline TiO_2 doped by 3d-metal ions. *Nanosystems: Physics, Chemistry, Mathematics*, 2018, **9**, P. 401–409.

[5] Kozlov D.A., Lebedev V.A., et al The microstructure effect on the Au/TiO_2 and Ag/TiO_2 nanocomposites photocatalytic activity. *Nanosystems: Physics, Chemistry, Mathematics*, 2018, **9**, P. 266–278.

[6] Szanyi J., Kwak J.H., Photo-catalytic oxidation of acetone on a TiO_2 powder: An in situ FTIR investigation. *Journal of Molecular Catalysis A: Chemistry*, 2015, **406**, P. 213–223.

[7] Ulyanova E.S., Zamyatin D.A., Kolosov V.Yu., Shalaeva E.V. Visible light photoluminescence in TiO_2/CdS nanopowders synthesized by sol-gel route: effect of gel aging time. *Nanosystems: Physics, Chemistry, Mathematics*, 2020, **11**, P. 480–487.

[8] Zavialova A.Yu., Bugrov A.N., et al Structure and photoluminescent properties of TiO_2:Eu^{3+} nanoparticles synthesized under hydro and solvothermal conditions from different precursors. *Nanosystems: Physics, Chemistry, Mathematics*, 2019, **10**, P. 361–373.

[9] Wang Y., Sun C.,et al. The Application of Nano-TiO_2 Photo Semiconductors in Agriculture. *Nanoscale Research Letters*, 2016, **11**, 529.

[10] Morozova P.A., Petukhov D.I. Preparation of Au/TiO_2/Ti memristive elements via anodic oxidation. *Nanosystems: Physics, Chemistry, Mathematics*, 2017, **8**, P. 823–829.

[11] Ganeshraja A.S., Anbalagan K. Participation of nanocrystalline TiO_2 Surface in the electron transfer between semiconductor solid and adsorbed cobalt(III)-RPY complex. *Nanosystems: Physics, Chemistry, Mathematics*, 2013, **4**, P. 276–287.

[12] Gazquez M.J., Bolivar J P., Garcia-Tenorio R., Vaca F. A review of the production cycle of titanium dioxide pigment. *Materials Sciences and Applications*, 2014, **5**, P. 441–458.

[13] Dimkpa C.O. Can nanotechnology deliver the promised benefits without negatively impacting soil microbial life. *Journal of Basic Microbiology*, 2014, **54**, P. 889–904.

[14] Peller J., Wies O., Kamat P.V. Hydroxyl Radical's Role in the Remediation of a Common Herbicide, 2,4-Dichlorophenoxyacetic Acid (2,4-D). *Journal of Physical Chemistry A*, 2004, **108**, P. 10925–10933.

[15] Hou J., Wang X., et al. Toxicity and mechanisms of action of titanium dioxide nanoparticles in living organisms. *Journal of environmental sciences (China)*, 2019, P. 7540–7553.

[16] Guan H.N., Chi D.F., Yu J., Li X.C. A novel photodegradable insecticide: preparation, characterization and properties evaluation of nano-Imidacloprid. *Pesticide Biochemistry and Physiology*, 2008, **92**, P. 83–91.

[17] Ahmed S., Rasul M.G., Brown R., Hashib M.A. Influence of parameters on the heterogeneous photocatalytic degradation of pesticides and phenolic contaminants in wastewater. *J. Environ. Manage*, 2011, **92**, P. 311–330.

[18] Parida K.M., Sahu N., et al. Preparation, characterization, and photo-catalytic activity of sulfate-modified titania for degradation of methyl orange under visible light. *J Colloid Interface Sci.*, 2008, **318**, P. 231–237.

[19] Aragay G., Pino F., Merkoç I.A. Nanomaterials for sensing and destroying pesticides. *Chemical Reviews*, 2012, **112**, P. 5317–5338.

[20] Lee K., Ku H., Pak D. OH radical generation in a photocatalytic reactor using TiO_2 nanotube plates. *Chemosphere*, 2016, **149**, P. 114–120.

[21] Devipriya S., Yesodharan S. Photocatalytic degradation of pesticide contaminants in water. *Solar Energy Materials & Solar Cells*, 2005, **86**, P. 309–348.

[22] Rabindranathan S., Devipriya S., Yesodharan S. Photocatalytic degradation of phosphamidon on semiconductor oxides. *Journal of Hazardous Materials*, 2003, **102**, P. 217–229.

[23] Lhomme L., Brosillon S., Wolbert D. Photocatalytic degradation of pesticides in pure water and a commercial agricultural solution on TiO_2 coated media. *Chemosphere*, 2008, **70**, P. 381–386.

[24] Marien C.B.D., Cottineau T., Robert D., Drogui P. TiO_2 nanotube arrays: influence of tube length on the photocatalyticdegradation of Paraquat. *Applied Catalysis B: Environmental*, 2016, **194**, P. 1–6.

[25] Bzdon S., Goralski J., et al. Radiation-induced synthesis of Fe-doped TiO_2: characterization and catalytic properties. *Radiation Physics and Chemistry*, 2012, **81**, P. 59–63.

[26] Attarchi N., Montazer M., Toliyat T. Ag/TiO_2/β-CD nano composite: preparation and photo catalytic properties for methylene blue degradation. *Applied Catalysis A: General*, 2013, **467**, P. 107–116.

[27] Zhang X., Wu F., et al. Photocatalytic degradation of 4,4'-biphenol in TiO_2 suspension in the presence of cyclodextrins: a trinity integrated mechanism. *Journal of Molecular Catalysis A: Chemistry*, 2009, **301**, P. 134–139.

[28] Ramos-Delgado N.A., Gracia-Pinilla M.A., et al. Solar photocatalytic activity of TiO_2 modified with WO3 on the degradation of an organophosphorus pesticide. *Journal of Hazardous Mater*, 2013, **263**, P. 36–44.

[29] Vamathevan V., Amal R., et al. Silver metallization of titania particles: effects on photoactivity for the oxidation of organics. *Journal of Gastrointestinal Surgery*, 2015, **19**, P. 1–6.

[30] Behnajady M.A., Modirshahla N., Hamzavi R. Kinetic study on photocatalytic degradation of C.I. acid yellow 23 by ZnO photocatalyst. *Journal of Hazardous Materials*, 2006, **133**, P. 226–232.

[31] Leghari S.A.K., Sajjad S., Chen F., Zhang J. WO3/TiO_2 composite with morphology change via hydrothermal template-free route as an efficient visible light photocatalyst. *Chemical Engineering Journal*, 2011, **166**, P. 906–915.

[32] Yao K.S., Wang D.Y., et al. Photocatalytic bactericidal effect of TiO_2 thin film on plant pathogens. *Surface & Coatings Technology*, 2007, **201**, P. 6886–6888.

[33] Yao K.S., Wang D.Y., et al. Photocatalytic disinfection of phytopathogenic bacteria by dye-sensitized TiO_2 thin film activated by visible light. *Surface & Coatings Technology*, 2007, **202**, P. 1329–1332.

[34] Cui H.X., Yang G.C., et al. Biological effects of PAS TiO_2 sol on disease control and photosynthesis in cucumber (Cucumis sativus L). *Australian Journal of Crop Science*, 2013, **7**, P. 99–103.

[35] Shilova O.A., Khamova T.V., et al. Synthesis and Research of Functional Layers Based on Titanium Dioxide Nanoparticles and Silica Sols Formed on the Surface of Seeds of Chinese Cabbage. *Russian Journal of Applied Chemistry*, 2020, **93** (1), P. 25–34.

[36] Khot L.R., Ehsani R., et al. Applications of nanomaterials in agricultural production and crop protection. A review. *Crop Protection*, 2012, **35**, P. 64–70.

[37] Zheng L., Hong F., Lu S., Liu C. Effect of nano-TiO_2 on strength of naturally aged seeds and growth of spinach. *Biological Trace Element Research*, 2005, **104**, P. 83–91.

[38] Song G., Gao Y., et al. Physiological effect of anatase TiO_2 nanoparticles on Lemna minor. *Environmental Toxicology and Chemistry*, 2012, **31**, P. 2147–2152.

[39] Yang F., Liu C., et al. The improvement of spinach growth by nano-anatase TiO_2 treatment is related to nitrogen photoreduction. *Biological Trace Element Research*, 2007, **119**, P. 77–88.

[40] Raliya R., Biswas P., Tarafdar J.C., TiO_2 nanoparticle biosynthesis and its physiological effect on mung bean (Vigna radiata L). *Biotechnology Reports*, 2015, **5**, P. 22–26.

[41] Palmqvist N.G.M., Bejai S., et al. Nano titania aided clustering and adhesion of beneficial bacteria to plant roots to enhance crop growth and stress management. *Scientific Reports*, 2015, **5**, 10146.

[42] Wang Y., Liu L., et al. Synthesis of Modified TiO_2 Nanoparticles with Polyacrylonitrile and Poly(hydroxyethyl acrylate) via ATRP. *Chemistry Select*, 2020, **5**, P. 4695–4700.

[43] Kopec M., Spanjers J., et al. Surface-initiated ATRP from polydopamine-modified TiO_2 nanoparticles. *European Polymer Journal*, 2018, **106**, P. 291–296.

[44] Ensafi A.A., Khoddami E., Nabiyan A., Rezaei B. Study the role of poly(diethyl aminoethyl methacrylate) as a modified and grafted shell for TiO_2 and ZnO nanoparticles, application in flutamide delivery. *Reactive & Functional Polymers*, 2017, **116**, P. 1–8.

[45] Park J.T., Lee C.S., Park C.H., Kim J.H. Preparation of TiO_2/Ag binary nanocomposite as high-activity visible-light-driven photocatalyst via graft polymerization. *Chemical Physics Letters*, 2017, **685**, P. 119–126.

[46] Maeda S., Fujita M., et al. Preparation of Transparent Bulk TiO_2/PMMA Hybrids with Improved Refractive Indices via an in Situ Polymerization Process Using TiO_2 Nanoparticles Bearing PMMA Chains Grown by Surface-Initiated Atom Transfer Radical Polymerization. *ACS Applied Materials & Interfaces*, 2016, **8**, P. 34762–34769.

[47] Mai T.B., Tran T.N., et al. Synthesis and characterization of poly(oligoethyleneglycol methacrylate)-g-TiO_2 nanocomposites via surface-initiated ARGET ATRP. *Molecular Crystals and Liquid Crystals*, 2014, **602**, P. 118–125.

[48] Liu L., Chen H., Yang F. Enhancing membrane performance by blending ATRP grafted PMMA-TiO_2 or PMMA-PSBMA-TiO_2 in PVDF. *Separation and Purification Technology*, 2014, **133**, P. 22–31.

[49] Zhang G., Lu S., et al. Novel polysulfone hybrid ultrafiltration membrane prepared with TiO_2-g-HEMA and its antifouling characteristics. *Journal of Membrane Science*, 2013, **436**, P. 163–173.

[50] Cui W.-W., Tang D.-Y., Gong Z.-L. Electrospun poly(vinylidene fluoride)/poly(methyl methacrylate) grafted TiO_2 composite nanofibrous membrane as polymer electrolyte for lithium-ion batteries. *Journal of Power Sources*, 2013, **223**, P. 206–213.

[51] Gong Z.-L., Tang D.-Y., Guo Y.-D. The fabrication and self-flocculation effect of hybrid TiO_2 nanoparticles grafted with poly(N-isopropylacrylamide) at ambient temperature via surface-initiated atom transfer radical polymerization. *Journal of Materials Chemistry*, 2012, **22**, P. 16872–16879.

[52] Chen H., Pan S., et al. Preparation of thermo-responsive superhydrophobic TiO_2/poly(N-isopropylacrylamide) microspheres. *Applied Surface Science*, 2012, **258**, P. 9505–9509.

[53] Xiong L., Liang H., Wang R., Chen L. A novel route for the synthesis of poly(2-hydroxyethyl methacrylate-co-methyl methacrylate) grafted titania nanoparticles via ATRP. *Journal of Polymer Research*, 2011, **18**, P. 1017–1021.

[54] Park J.T., Koh J.H., et al. Proton-conducting nanocomposite membranes based on P(VDF-co-CTFE)-g-PSSA graft copolymer and TiO_2-PSSA nanoparticles. *International Journal of Hydrogen Energy*, 2011, **36**, P. 1820–1827.

[55] Akpolat L.B., Cakir B.A., Topel O., Hoda N. Synthesis of TiO_2 nanoparticles by self-assembling reverse micelle cores of PS-b-PAA for functional textile applications. *Materials Research Bulletin*, 2015, **64**, P. 117–122.

[56] Shilova O.A., Panova G.G., et al. Properties, and Phytoprotective Functions of Titanium Dioxide Nanopowders and Their Aqueous Suspensions. *Russian Journal of Inorganic Chemistry*, 2021, **66**, P. 765–772.

[57] Mueller R., Kammler H.K., Wegner K., Pratsinis S.E. OH Surface Density of SiO_2 and TiO_2 by Thermogravimetric Analysis. *Langmuir*, 2003, **19**, P. 160–165.

[58] Ou B., Li D., et al. Functionalized TiO_2 nanoparticle containing isocyanate groups. *Material Chemistry and Physics*, 2012, **135**, P. 1104–1107.

[59] Zhao J., Milanova M., Warmoeskerken M.M.C.G., Dutschk V. Surface modification of TiO_2 nanoparticles with silane coupling agents. *Colloids and Surfaces A: Physicochemical and Engineering Aspects*, 2012, **413**, P. 273– 279.

[60] Yakimansky A.V., Meleshko T.K., et al. Novel Regular Polyimide-graft-Poly(methacrylic acid) Brushes: Synthesis and Possible Applications as Nanocontainers of Cyanoporphyrazine Agents for Photodynamic Therapy. *Journal of Polymer Science, Part A: Polymer Chemistry*, 2013, **51**, P. 4267–4281.

[61] Kashina A.V., Meleshko T.K., et al. Synthesis of Pentablock Copolymers of the Mixed Linear-Brush Topology by Controlled Radical Polymerization and Ring-Opening Polymerization Reactions. *Polymer Science, Series C*, 2019, **61**, P. 174–185.

[62] Pugachevskii M.A. Ultraviolet absorption spectrum of laser-ablated titanium dioxide nanoparticles. *Technical Physics Letters*, 2013, **39**, P. 36–38.

[63] Raghuraman G.K., Rühe J., Dhamodharan R. Grafting of PMMA brushes on titania nanoparticulate surface via surface-initiated conventional radical and “controlled” radical polymerization (ATRP). *Journal of Nanoparticle Research*, 2008, **10**, P. 415–427.